# An excited state of <sup>229</sup>Th at 3.5 eV

R. G. Helmer and C. W. Reich Idaho National Engineering Laboratory, EG&G Idaho, Inc., Idaho Falls, Idaho 83415 (Received 8 October 1993)

It has been known for many years that the first excited state of <sup>229</sup>Th lies close to the ground state. Originally this energy was given as < 0.1 keV; later, the authors reported a value of  $-1 \pm 4$ eV. In an attempt to improve the value for this level energy, we have remeasured the energies of a number of  $\gamma$  rays from <sup>233</sup>U whose positions in the <sup>229</sup>Th level scheme can be used to establish it. Compared with our earlier study, we have considered more  $\gamma$  rays in <sup>229</sup>Th, used more well-measured energy calibration and reference lines, used more detectors, used detectors with better low-energy resolution, more closely matched the counting rates in the  $\gamma$ -ray peaks whose relative energy is measured, and specifically considered certain systematic errors. More than 111  $\gamma$ -ray spectra have been measured. From this large set of measurements we have deduced a value of  $3.5 \pm 1.0$  eV for the energy of this level.

#### PACS number(s): 23.20.Lv, 27.90.+b

# I. INTRODUCTION

In a study of the level structure of <sup>229</sup>Th from the  $\alpha$  decay of  $^{233}$ U, Kroger and Reich [1] concluded that the first excited state in <sup>229</sup>Th, which has  $J^{\pi} = 3/2^{+}$ , occurs within 0.1 keV of the 5/2+ ground state. More recently, Reich and Helmer [2] reported measurements of  $\gamma$ -ray energy differences from which they deduced that this level energy is  $-1 \pm 4$  eV. Since it is presumed [2] that the  $3/2^+$  state lies above the  $5/2^+$  state, this result can also be stated as indicating that this excited level lies below 7 eV (at the  $2\sigma$  level).

The existence of an excited nuclear state at such a low energy, especially one that is connected to the ground state via an M1 transition, presents an opportunity to investigate a variety of interesting phenomena related to the interaction of the nucleus with its electronic environment. A number of novel, nonnuclear ways of exciting this level could be studied. Included among these would be excitation of the electron cloud from an external source (e.g., a laser or thermal means) with subsequent energy transfer to the nucleus. With an energy below that of the most loosely bound atomic electron in thorium ( $\sim 5.5 \text{ eV}$ ), the decay of the excited state may not be able to proceed via internal conversion, but it might excite transitions between bound atomic levels. With its sensitivity to the electronic structure, the lifetime of this state is expected to depend on the chemical (and physical) state of the material in which the <sup>229</sup>Th is imbedded; and, conversely, measurements of this lifetime in different chemical and physical environments could provide interesting information for atomic and condensed-matter physics. In fact, since the initial report [2] of the uniquely low energy for this state, a rather extensive literature regarding it has grown up, and continues to grow (see, e.g., Refs. [3-9]).

Because of the interest in this particular level, we undertook a new series of measurements in an attempt to obtain a value, rather than simply a limit, for its energy. We did this by determining more precise energies for some of the  $\gamma$  rays from the decay of <sup>233</sup>U that involve this level. The relationships of the  $\gamma$  rays involved in these measurements are shown in Fig. 1. The energy,  $\Delta$ , of the first excited level is given by each of the four combinations of  $\gamma$ -ray energies:

$$\Delta = 97.1 - 25.3 - 71.8,$$

$$\Delta = 97.1 - 67.9 - 29.1,$$

$$\Delta = 148.1 - 118.9 + 117.1 - 146.3$$

and

$$\Delta = 148.1 - 76.4 + 74.6 - 146.3$$
.

Also of interest are the two cascade-crossover combina-

$$217.1 = 187.9 + 29.1$$

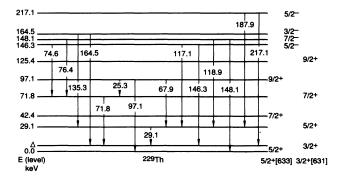


FIG. 1. A portion of the low-energy level scheme of <sup>229</sup>Th showing the  $\gamma$  rays that are used in this determination of the energy  $\Delta$  of the first excited level.

49

and

$$164.5 = 135.3 + 29.1.$$

The extent to which the measured  $\gamma$ -ray energies do not satisfy these two relationships provides a measure of possible systematic errors.

The present measurements differ from those reported previously [2] in the following ways:

- (i) more  $\gamma$  rays in <sup>229</sup>Th were considered;
- (ii) measurements were made on five detectors rather than only one;
  - (iii) more reference lines were used for calibration;
- (iv) more measurements were made for each energy difference:
  - (v) detectors with better energy resolution were used;
- (vi) the activities of the calibration and <sup>233</sup>U sources were carefully matched, so they could be mounted adjacent to each other and thereby reduce the systematic errors due to peak shifts with source position [10]; and

(vii) the peak fitting was done on an interactive system. In this paper, we describe the methods used (Sec. II); the measurement of the energies for some  $\gamma$  rays from <sup>233</sup>U (Sec. III); and the use of these results to determine the level energy in <sup>229</sup>Th (Sec. IV). A brief discussion of the result and its implications is given in Sec. V. For completeness, and for possible future use, all of the energy values obtained in this study are reported even though many of them are not applicable to the <sup>229</sup>Th level-energy determination. Because of the large number of measurements carried out and the exhaustive nature of the data analysis, most of the details of the actual experimental analyses are not given here. They are contained in a separate laboratory report [11] which can be made available to those wanting a more complete discussion of the experimental procedures and data analysis.

# II. METHODOLOGY

#### A. Energy scale and uncertainties

The  $\gamma$ -ray energies reported here are based on the scale used for the IUPAP-recommended list of energies [12]. On this scale the primary  $\gamma$  ray from the decay of  $^{198}\mathrm{Au}$ has an energy of 411.8044(11) keV. The energy of this line has been determined from very precise measurements of its wavelength [13]. If one were to adjust the eV energy scale to correspond to the most recent values of this wavelength and the fundamental constants, the energy of this 411-keV line would be reduced by 5.8 ppm. Most of the other calibration lines used here would consequently also be reduced by a similar amount. This small change would not influence our final results and, therefore, this correction has not been made. For our work here, we need consider only the measurement uncertainties for the calibration lines used. That is, we can do all the energy comparisons on what is effectively the wavelength scale. In this way, the measurements relative to different reference lines are properly weighted. In principle, the uncertainty in the conversion between the wavelength and eV scales should be added back in for the final result. But, since the measurement uncertainty in our final result is of the order of 15%, this uncertainty is not significant and has not been considered further.

### B. Calibration sources

In the search for radionuclides that provide  $\gamma$ -ray lines that would be useful as reference lines, there were two criteria. First, the  $\gamma$ -ray energies should be very well known. Ideally, this means that the uncertainty in the energy is < 1 eV and that its measurement was made in the last 15 years or so. Second, the reference lines should be near to, but resolved from, each of the  $\gamma$  rays of interest from  $^{233}$ U.

The energy-calibration sources used were  $^{172}{\rm Hf} + ^{172}{\rm Lu},$   $^{161}{\rm Tb},~^{241}{\rm Am},~^{182}{\rm Ta},~^{169}{\rm Yb},~^{152}{\rm Eu},~^{210}{\rm Pb},~{\rm and}~^{170}{\rm Tm}.$ The energies of the  $\gamma$  rays used are given in Table I. Among these lines, those for <sup>172</sup>Hf+<sup>172</sup>Lu and <sup>241</sup>Am were measured [14] specifically for this study. The <sup>241</sup>Am lines were remeasured because the previous values did not meet the above criteria: these values [19,20] had uncertainties of 1 eV; and the measurements are old (i.e., 1968 and 1970). The values for  $^{172}$ Hf  $(1.87 \text{ y})+^{172}$ Lu were measured to allow the use of the 23.9Hf line as an intermediate reference line between the 25.6Tb line and the 25.3U line. (The notation 25Tb means the 25-keV line from the decay of <sup>161</sup>Tb. The notation used to denote the radionuclides is: <sup>152</sup>Eu, Eu; <sup>161</sup>Tb, Tb; <sup>169</sup>Yb, Yb; <sup>170</sup>Tm, Tm; <sup>172</sup>Hf+<sup>172</sup>Lu, Hf; <sup>182</sup>Ta, Ta; <sup>210</sup>Pb, Pb, <sup>233</sup>U, U; and <sup>241</sup>Am, Am.) The only remaining line that does not meet the above criteria is that for <sup>210</sup>Pb, which is from Helmer et al. [15] and is known to only 1 eV. The radionuclides listed in Table I have many other  $\gamma$  rays with well-measured energies, but these lines were either not in an energy range of interest or there were <sup>233</sup>U lines which interfered with their use.

The use of the 25.6Tb line as a reference line is somewhat complicated, since this line is not resolved from the 25.3U line, whose energy we wish to determine. Therefore, we have had to make use of a two-step process to determine this 25.6Tb-25.3U energy difference. <sup>172</sup>Hf has a strong line at 23.9 keV, so we measured the 23.9Hf-25.6Tb difference to obtain the energy of the <sup>172</sup>Hf line. From this and the measured 23.9Hf-25.3U difference, we obtained the energy of the <sup>233</sup>U line. Similarly, the 25.6Tb-26.3Am difference was used to determine the energy of the <sup>241</sup>Am line, and the 25.3U-26.3Am difference gives another measurement of the energy of the <sup>233</sup>U line.

The calibration sources were prepared by depositing a solution containing the radionuclide onto a backing of polyimide film, drying the solution, and covering it with tape and polyimide film. In most cases, sources were made with a range of activities. The <sup>233</sup>U sources were also made with a range of activities. This variety of source strengths was necessary so the <sup>233</sup>U and calibration sources could be paired in such a way as to have similar peak counting rates for the lines to be compared, and still have the sources be adjacent to each other. In all

cases the source holders were in contact, so the sources were separated by distances of  $\sim 0.3$  cm.

## C. Measurement and analysis methods

The typical measurement procedure can be illustrated for the case where the energy of the 42U line is compared with that of the 46Pb line. Particular sources of  $^{233}\mathrm{U}$  and  $^{210}\mathrm{Pb}$  were chosen so that the count rates in these two peaks were comparable when the sources were placed adjacent to each other. A source-to-detector distance of 10 cm was typically chosen so that the sources were "far" from the detector compared to the difference in the source position ( $\sim 0.3$  cm), but still gave a sufficient counting rate. Half of the measured spectra were obtained with the  $^{233}\mathrm{U}$  source nearer the detector and the other half with the  $^{210}\mathrm{Pb}$  source nearer the detector; this would cancel out any bias in the energy difference due to differences in the source-detector distances. Since  $^{210}\mathrm{Pb}$  has only one  $\gamma$  ray, most of the calibration lines used were from  $^{233}\mathrm{U}$ .

In the analysis of these spectra, the energy-channel relationship was taken to be

$$E(x) = a + b(x - \delta) + c(x - \delta)^{2}$$

where x is the channel and E is the energy. The parameters a, b, and c were determined by a least-squares fit to the energies and positions of these peaks. The parameter  $\delta$  is an estimated zero offset that is computed separately before the parameters a, b, and c are computed. In this step the routine automatically defines the peak fitting region for each peak; that is, the fitting is not interactive.

An interactive routine was then used to fit the peaks of interest in determining  $\gamma$ -ray energy differences. In this peak-fitting routine the user identifies, on a video screen, the channels below and above the peak to be used to determine the linear or step background function, the channel range included in the fit of the peak parameters, and the initial centroid of the peak. The peak parameters are then calculated by a nonlinear least-squares routine.

The peak positions,  $X_1$  and  $X_2$ , from these fits are then used to determine the difference in energy between nearby peaks, namely,

$$\Delta E = E_2 - E_1 = b(X_2 - X_1) + c(X_2^2 - X_1^2).$$

The calculation of the uncertainty in this difference

TABLE I. Energies of reference and calibration lines. Uncertainties include only those from the measurement and not that from the conversion between the wavelength and eV energy scales (see text).

Parent		Parent	
isotope	Energy (keV)	isotope	${\bf Energy} \; ({\bf keV})$
<sup>172</sup> Hf+ <sup>172</sup> Lu <sup>a</sup>	23.9331(2)	<sup>210</sup> Pb <sup>b</sup>	46.539(1)
	78.7426(6)		,
$^{161}\mathrm{Tb^c}$	25.65150(3)	$^{169}\mathrm{Yb^d}$	63.12077(8)
	48.91562(6)		109.77987(5)
	74.56711(10)		130.52368(4)
			177.21402(6)
			197.95788(6)
<sup>241</sup> Am <sup>a</sup>	26.3448(2)		261.07857(11)
	59.5412(2)		307.73757(9)
$^{182}\mathrm{Ta^e}$	31.7378(7)		
	84.6808(3)	$^{170}\mathrm{Tm^f}$	84.25510(19)
	100.10653(18)		, ,
	113.6723(2)		
	152.4308(3)	$^{152}\mathrm{Eu^g}$	344.2811(17)
	156.3874(3)		
	179.3948(3)		
	198.3530(3)		
	222.1099(3)		
	229.3220(6)		
	264.0755(3)		

<sup>&</sup>lt;sup>a</sup>Energies from Ref. [14] and were measured for this study.

<sup>&</sup>lt;sup>b</sup>Energy from Ref. [15].

<sup>&</sup>lt;sup>c</sup>Energy from Ref. [16].

<sup>&</sup>lt;sup>d</sup>Energies from Ref. [17].

<sup>&</sup>lt;sup>e</sup>Energies from Ref. [12], except for the 31-keV  $\gamma$  ray, which is computed from the 116.4186(6)-84.6808(3) difference.

<sup>&</sup>lt;sup>f</sup>Energy from Ref. [12].

<sup>&</sup>lt;sup>g</sup>Energy from Ref. [12]. See also Ref. [18].

includes the variances in b, c,  $X_1$ , and  $X_2$  and the covariance between b and c. This uncertainty is dominated by the two terms involving  $var(X_1)$  and  $var(X_2)$ .

For each energy difference where data were taken on different detectors, weighted averages were computed for each detector separately, and for all of the data together. The reduced- $\chi^2$  value,  $\chi^2_R$ , was determined for each average. If the  $\chi^2_R$  values were larger than expected, or the averages from different detectors were inconsistent, the data were reviewed to determine if there was an identifiable problem. In some cases a single value, which was an extreme outlier, was removed and the averages recalculated.

The uncertainties given throughout this work, except as influenced by the  $\chi^2_R$  values, are statistical only. Some potential sources of systematic error were considered but finally not included because of the following considerations.

In fitting a set of calibration lines, we used a quadratic relationship  $E_q(X)$  between the energy and the channel number, which will differ from the true relationship  $E_t(X)$  by an amount  $\delta E(E\gamma)$ . There are several contributions to this difference: (i) the statistical variations in the peak locations; (ii) any errors (not uncertainties, but actual errors) in the calibration energies; and (iii) the fact that the true relationship may not be adequately represented by any quadratic function (i.e., the true relationship has higher-order terms). In addition to these general contributions, for an individual  $\gamma$ -ray peak a fourth factor would be any shift in its position due to other peaks in the spectrum. In our computation of an energy difference  $\Delta E$  between two lines from one spectrum, all of these factors are ignored.

Before discussing our method of addressing these four factors, let us note the precision we are implying in our results. The smallest uncertainty that we have quoted for an average  $\Delta E$  is 0.1 eV. Since this is from more than

16 measurements, this corresponds to an uncertainty of about 0.4 eV for an individual measurement, if each measured value has the same uncertainty. Many measurements were made with a gain scale corresponding to 20 eV per channel. An uncertainty in a peak position of 0.4 eV then corresponds to 0.02 channels. It is questionable if  $\delta E(E\gamma)$  is this small. However, since we are always determining an energy difference, it is actually only the change in  $\delta E(E\gamma)$  between the two peak positions that needs to be this small.

Our decision to quote only the statistical uncertainty is based on the following. It is assumed that, since the first factor mentioned above is statistical, in an average over many spectra it will be averaged out. It is assumed that the second contribution will be identified, or at least partially averaged out by using different calibration lines whenever possible.

We chose to treat the third factor by making our measurements in the following manner. Each measurement was made on a different gain scale, and measurements were made on different detectors, each with its own analog-to-digital converter (ADC) and amplifier. Both of these variations in the experimental setup are expected to result in different functions  $\delta E(E\gamma)$ . It is assumed that by averaging the results from all of the measurements the average  $\delta E$  will approach zero.

The fourth factor must be dealt with individually for each peak for which it was a concern. A case of particular interest is the 25Tb-26Am difference. Since these peaks are not completely resolved, as shown in Fig. 2, in fitting one of these peaks, the second peak will tend to move the apparent peak location of the first peak closer to that of the second one. Therefore, the measured difference is expected to be less than the actual one. If this effect is significant, the observed difference should increase as the detector resolution improves. In fact, the values from the Si(Li) and OR-16 detectors agree very

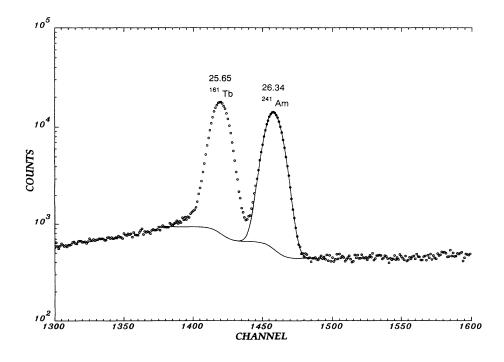


FIG. 2. Portion of the  $^{161}$ Tb and  $^{241}$ Am  $\gamma$ -ray spectrum measured with the OR-16 detector showing the  $\gamma$  rays at 25.65 and 26.34 keV. The solid curves show spectral background used in the fit to the 26.34-keV peak and the Gaussian plus background from the fit.

TABLE II. Properties of detectors.

			Volume	Diam.	Depth	FWHM	(eV) at
Detector	Material	$\mathbf{Shape}$	$(cm^3)$	(mm)	(mm)	$29~{ m keV}$	122 keV
OR-12	Ge	coaxial	114				950
PG-21	$\mathbf{Ge}$	coaxial	63				900
PG-16	Ge	planar		16	10	390	
OR-16	Ge	planar		10	7	270	
Si	Si(Li)	planar		6	4	345	

well, so this effect is believed to be negligible. Thus, all of these measurements have been used.

#### D. Detectors

Some properties of the five detectors used in this study are given in Table II. The detectors include two high-purity Ge coaxial detectors, two Ge planar detectors, and a Si(Li) detector. The resolutions given in the table are not the optimum values for these detectors; rather, they are observed values for actual spectra, where the counting times were typically 72 hours.

# III. MEASUREMENT RESULTS AND $\gamma$ -RAY ENERGIES FOR <sup>288</sup>U

#### A. Measurement results

A total of 111 spectra were measured for this study. The individual values for all of the energy differences deduced from these spectra are given in Ref. [11] and the ones used herein are given in Table III. As illustrations of the spectra obtained, Figs. 2–4 show portions of the  $\gamma$ -ray spectra from two of the detectors. These figures show the quality of the data obtained, that is, the typical counting statistics and the resolution obtained. (See Ref. [11] for figures showing peaks in other energy regions.)

From Fig. 3 it is clear that the 97-keV peak from <sup>233</sup>U includes several interfering lines, both at lower and higher energies. These lines, whose influence was not specifically taken into account in the analysis, may introduce a significant systematic error into the determination of the peak position of the 97-keV peak and hence into the measurement of 97U-100Ta energy difference, especially since the statistical uncertainty in this difference is only 0.3 eV, one of the smallest reported in this study. In order to investigate the possible magnitude of such an effect, four fits were made to this peak successively adding two channels (one on each side of the peak) to the fitting range, as shown in Table IV. The smallest fitting range, 9 channels, corresponds to the full width at half maxi-

TABLE III. Averages for measured  $\gamma$ -ray energy differences between lines from <sup>233</sup>U. See Ref. [11] for comments on values excluded from averages.

			Average	
		N 1 0	energy	
Lines		Number of	difference	_
(keV)	Detector	values	$(\mathrm{keV})$	$\chi^2_R$
25-29	PG-21	2	3.8947 (119)	0.47
	PG-16	15	3.8738 (13)	1.37
	OR-16	28	3.8691 (3)	1.21
	Si(Li)	17	3.8760 (11)	1.52
	All	62	3.8701 (4)	2.39
67-71	PG-16	27	3.8702 (7)	1.05
	OR-16	19	3.8679(4)	1.27
	Si(Li)	8	3.8612 (24)	0.93
	All	54	3.8685 (4)	1.45
117-118	OR-12	4	1.8127 (16)	2.91
	PG-21	4	1.8101 (26)	1.79
	PG-16	30	1.8094 (4)	1.07
	OR-16	25	$1.8089\ (2)$	0.79
	Si(Li)	8	1.8107(20)	0.45
	All	71	1.8092 (2)	0.96
146-148	PG-16	33	1.8145 (10)	1.77
	OR-16	16	1.8119 (8)	1.87
	All	49	1.8128(6)	1.91

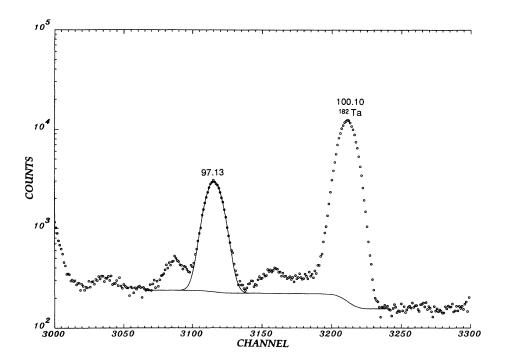


FIG. 3. Portion of the  $^{233}\mathrm{U}$  and  $^{182}\mathrm{Ta}$   $\gamma$ -ray spectrum measured with the OR-16 detector showing the  $\gamma$  rays at 97.13 and 100.10 keV.

mum (FWHM). In the analyses of the  $\gamma$ -ray peaks in this work, the fits are generally similar to the first two fitting ranges in this table. Similarly, four fits were made to the 100-keV peak from <sup>182</sup>Ta in the same spectrum.

Since we fit the peaks with a symmetric Gaussian function, we expect the calculated peak position to shift to lower values as more channels are included on the lowenergy side of any singlet peak. If the secondary peak on the low-energy side of the 97-keV line has any significant additional influence on the position of the main peak, we expect the shift of the calculated position of the 97-keV peak to be larger than that of the more nearly singlet

peak at 100 keV. The data in Table IV show that there is no significant difference in the shifts observed between these two peaks as the fitting range is increased. From this, we conclude that any influence on the calculated position of the 97-keV peak due to the presence of the peaks underlying it is less than about 0.5 eV.

In Fig. 4, a pair of important peaks, at 146 and 148 keV, is shown. The 148-keV peak has the difficulties that it is relatively weak, so it is hard to get good counting statistics, and that there is a small distortion on the low-energy side. In this case, the contribution of this peak to the uncertainty of the  $\gamma$ -ray energy difference should be

TABLE IV. Shifts in calculated peak positions as the fitting range is increased.

$\gamma ext{-ray}$	$\operatorname{Pe}{\mathbf{a}}{\mathbf{k}}$			No. of	Change in pe	eak position
energy (keV)	Channel	Area	$\chi^2_R$	channels in fit	Channels	eV
97	1618.0	16 100	≤ 1 <sup>a</sup>	9	≡0.000	≡0.0
			$\leq 1^{\mathbf{a}}$	11	-0.014	-0.8
			$\leq 1^{\mathbf{a}}$	13	-0.035	-2.1
			$ \leq 1^{\mathbf{a}} $	15	-0.039	-2.3
100	1667.6	16 200	$\leq 1^{\mathbf{a}}$	9	≡0.000	≡0.0
			$\leq 1^{\mathbf{a}}$	11	-0.013	-0.8
			$\leq 1^{\mathbf{a}}$	13	-0.022	-1.3
			$egin{array}{l} \le 1^{\mathbf{a}} \\ \le 1^{\mathbf{a}} \\ \le 1^{\mathbf{a}} \\ \le 1^{\mathbf{a}} \end{array}$	15	-0.033	-2.0
146	2365.9	248 000	$\leq 1^{\mathtt{a}}$	11	≡0.000	≡0.0
			$egin{array}{l} \leq 1^{\mathbf{a}} \ \leq 1^{\mathbf{a}} \ 2.3 \end{array}$	13	-0.009	-0.6
			2.3	15	-0.049	-3.0
			3.2	17	-0.082	-5.1
152	2464.4	287 000	1.5	12	<b>≡0.000</b>	≡0.0
			2.2	14	-0.036	-2.2
			2.5	16	-0.055	-3.4
			2.6	18	-0.073	-4.5

<sup>&</sup>lt;sup>a</sup>For values < 1.0, the computer program does not give explicit values.

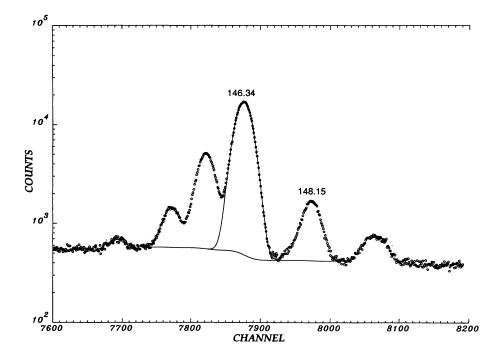


FIG. 4. Portion of the  $^{233}$ U  $\gamma$ -ray spectrum measured with the OR-16 detector showing the  $\gamma$  rays at 146.34 and 148.15 keV.

dominated by this statistical component. The 146-keV peak has the problem of the presence of the 145-keV line. Only the top portions of the peaks are used in the fit to a singlet, and a Gaussian function without any tailing is used in the fit. If one were to fit the 145-146 pair as a doublet, one would include portions of each peak all the way down to the spectral background; and this would produce an unacceptable bias between the fits to 146- and 148-keV peaks. Therefore, a singlet fit to the 146-keV peak was preferred.

As discussed above in regard to the 97-keV peak, we have explored the change in the computed positions of the 146- and 152-keV peaks in the spectrum of  $^{233}\mathrm{U}$  and  $^{152}\mathrm{Eu}$  in order to investigate the presence of possible systematic errors in the calculated position of the 146-keV peak due to the presence of the near-lying 145-keV  $\gamma$  peak (which was not specifically included in the analysis). We assume that any influence of the 145-keV peak would cause the shift in the calculated 146-keV peak position to be larger than that for the 152-keV peak, which is a singlet. As shown in Table IV, no such effect is seen. Therefore, we conclude that any such influence is less than about 0.5 eV.

Since all four values of  $\Delta$  discussed in Sec. IV depend on either the 97-keV  $\gamma$ -ray energy or the 146-148 energy difference, our results depend critically on the fits to the lines in Figs. 3 and 4.

# B. $\gamma$ -ray energies

From the energy differences in Ref. [11], the energies for many of the  $\gamma$  rays from <sup>233</sup>U have been deduced. These results are given in Table V.

In considering these results, it should be understood that these energies have been determined by doing the calculations in a particular order. In some instances, the calculations could have been done in a different order, in which case some of the  $\gamma$ -ray energies would have been slightly different. To illustrate, assume we have the following set of data:

Calibration line energies:

$$C_1$$
 and  $C_2$  with  $C_1 < C_2$ .

 $\gamma$  energies to be determined:

$$E_1$$
 and  $E_2$  with  $C_1 < E_1 < E_2 < C_2$ .

Measurement results:

$$\Delta_1(E_1-C_1), \ \Delta_2(E_2-E_1), \ \text{and} \ \Delta_3(C_2-E_2).$$

Then one can determine  $E_1$  and  $E_2$  from either of the following two sets of relationships:

$$E_1 = C_1 + \Delta_1 \text{ and}$$
 (1)

 $E_2$  is the average of  $C_1 + \Delta_1 + \Delta_2$  and  $C_2 - \Delta_3$ ,

 $\mathbf{or}$ 

$$E_2 = C_2 - \Delta_3$$
 and (2)

$$E_1$$
 is the average of  $C_1 + \Delta_1$  and  $C_2 - \Delta_3 - \Delta_2$ .

It would, of course, be possible to remove this bias of choosing a particular order for the calculations by doing a least-squares fit to each of the over determined sets of data. To do such a fit correctly one would need to develop a covariance matrix for the measured  $\Delta_i$  values because generally they will be highly correlated. For ex-

TABLE V.  $\gamma$ -ray energies for  $^{233}\mathrm{U}$  lines.

<sup>233</sup> U	Reference		${f Adopted}$	$\gamma$ -ray energy		
line	Nuclide	Energy	$\Delta E_{\gamma}$	Value	Average	$\chi^2_R$
25	<sup>241</sup> Am	26.3448(2)	1.0340(9)	25.3108(9)	25.3106(8)	0.15
	<sup>172</sup> Hf	23.9331(2)	1.3771(16)	25.3101(16)	2010100(0)	0.10
29	$^{182}\mathrm{Ta}$	31.7378(7)	2.5482(10)	29.1896(12)	29.1846(30)ª	12.9
20	<sup>172</sup> Hf	23.9331(2)	5.2489(9)	29.1820(9)	20.1010(00)	12.0
	<sup>241</sup> Am	26.3448(2)	2.8397(4)	29.1845(5)		
		, ,		. ,		
42	<sup>210</sup> Pb	46.539(1)	4.0862(6)	42.453(1)	$42.4524(7)^{\mathrm{b}}$	4.27
	$^{182}\mathrm{Ta}$	31.7378(7)	10.7181(9)	42.4559(11)		
	$^{161}{ m Tb}$	48.91562(6)	6.4642(4)	42.4518(4)		
	<sup>233</sup> U	54.7038(7)	12.2510(4)	42.4528(15)		
53	$^{210}\mathrm{Pb}$	46.539(1)	7.0708(12)	53.610(2)	53.6107(11)	0.20
	$^{233}\mathrm{U}$	54.7038(7)	$1.0927(3)^{'}$	53.6111(14)	,	
F 4	$^{210}{ m Pb}$	40 520(1)	0.1040(5)	F 4 709(1)	F 4 7020(14)8	0.63
54	<sup>241</sup> Am	46.539(1)	8.1640(5)	54.703(1)	$54.7038(14)^{\mathrm{a}}$	9.63
	169Yb	59.5412(2)	4.8374(2)	54.7036(4)		
	$^{161}\mathrm{Tb}$	63.1208(1)	8.4202(7)	$54.7006(7) \\ 54.7046(3)$		
	16	48.91562(6)	5.7890(3)	54.7040(5)		
66	$^{241}\mathrm{Am}$	59.5412(2)	6.5777(6)	66.1189(6)	66.1184(6)	1.69
	$^{169}\mathrm{Yb}$	63.1208(1)	2.9968(8)	66.1176(8)		
67	$^{241}\mathrm{Am}$	59.5412(2)	8.4048(12)	67.9460(12)	67.9460(5)	0.00
0.	$^{169}\mathrm{Yb}$	63.1208(1)	4.8252(10)	67.9460(10)	01.0100(0)	0.00
	<sup>233</sup> U	66.1184(6)	1.8276(4)	67.9460(7)		
	160					
70	<sup>169</sup> Yb	63.1208(1)	7.1614(16)	70.2822(16)	70.2813(13)	0.90
	$^{233}{ m U}$	71.8159(20)	1.5362(6)	70.2797(21)		
71	$^{241}\mathrm{Am}$	59.5412(2)	12.2719(10)	71.8131(10)	$71.8159(20)^{a}$	9.97
	$^{169}{ m Yb}$	63.1208(1)	8.6947(4)	71.8155(4)	, ,	
	$^{161}{ m Tb}$	74.56711(10)	2.7492(6)	71.8179(6)		
74	$^{182}\mathrm{Ta}$	84.6808(3)	10.1273(24)	74.5535(24)	74.5390(40) <sup>a</sup>	13.5
14	$^{170}\mathrm{Tm}$	84.2551(2)	9.7172(6)	74.5339(24) 74.5379(6)	14.0000(40)	10.0
	233	71.8159(20)	2.7242(3)	74.5401(20)		
	<sup>233</sup> U	76.3507(27)	1.8099(8)	74.5401(20) $74.5408(28)$		
		` ,	· /	, ,		
76	$^{182}\mathrm{Ta}$	84.6808(3)	8.3218(49)	76.359(5)	76.3507(27)	3.07
	$^{170}\mathrm{Tm}$	84.2551(2)	7.9053(16)	76.3498(16)		
83	$^{170}\mathrm{Tm}$	84.2551(2)	1.2423(20)	83.0128(20)		
85	$^{170}\mathrm{Tm}$	84.2551(2)	1.1673(17)	85.4224(17)		
88	$^{170}\mathrm{Tm}$	84.2551(2)	4.2195(14)	88.4746(14)		
89	$^{170}\mathrm{Tm}$	84.2551(2)	5.6995(5)	89.9546(5)	89.9568(24) <sup>a</sup>	15.9
	$^{182}\mathrm{Ta}$	84.6808(3)	5.2785(10)	89.9593(10)		
	$^{233}{ m U}$	93.3502(3)	$3.3924(3)^{'}$	$89.9578(4)^{'}$		
93	$^{233}{ m U}$	97.1344(3)	3.7842(1)	93.3502(3)		
97	$^{182}\mathrm{Ta}$	100.1065(2)	2.9721(2)	97.1344(3)		
117	<sup>182</sup> Ta	113.6723(2)	3.4905(12)	117.1628(12)	117.1628(9)	0.00
TTI	<sup>233</sup> U	118.9721(15)	1.8092(2)	117.1629(12) $117.1629(15)$		2.00

TABLE V. (Continued).

$^{233}\mathrm{U}$	R	eference	Adopted	$\gamma$ -ray	energy	
line	Nuclide	Energy	$\Delta \hat{E}_{\gamma}$	Value	Average	$\chi_R^2$
118	<sup>182</sup> Ta	113.6723(2)	5.2973(12)	118.9696(12)	118.9721(15)	5.99
110	<sup>233</sup> U	120.8194(7)	1.8464(2)	118.9730(7)	110.9721(13)	5.99
120	<sup>169</sup> Yb	120 5027(0)	0.7020(12)	100 0001(10)	100.0104(7)	0.40
120	<sup>233</sup> U	130.5237(0)	9.7036(13)	120.8201(13)	120.8194(7)	0.43
	_	135.3393(5)	14.5202(6)	120.8191(8)		
123	<sup>169</sup> Yb	130.5237(0)	6.6370(13)	123.8867(13)	123.8860(7)	0.43
	$^{233}\mathrm{U}$	120.8194(7)	3.0663(4)	123.8857(8)		
135	<sup>169</sup> Yb	130.5237(0)	4.8156(5)	135.3393(5)		
139	<sup>169</sup> Yb	130.5237(0)	9.2135(50)	139.7372(50)	139.7278(45)	4.37
	$^{233}\mathrm{U}$	135.3393 (5)	4.3863(23)	139.7256(24)	, ,	
146	<sup>169</sup> Yb	130.5237(0)	15.8228(25)	146.3465(25)	146.3462(6)	0.06
	$^{182}\mathrm{Ta}$	152.4308(3)	$6.0848(7)^{'}$	$146.3460(8)^{'}$		
	$^{182}\mathrm{Ta}$	156.3874(3)	10.0410(8)	146.3464(9)		
164	<sup>169</sup> Yb	177.2140(1)	12.6905(10)	164.5235(10)	164.5240(5)	0.27
	$^{182}\mathrm{Ta}$	152.4308(3)	12.0932(8)	164.5240(9)	101.0210(0)	0.21
	$^{182}\mathrm{Ta}$	156.3874(3)	8.1372(9)	164.5246(9)		
	$^{182}\mathrm{Ta}$	179.3948(3)	14.8711(9)	164.5237(9)		
169	$^{169}\mathrm{Yb}$	177.2140(1)	8.2123(54)	169.002(5)		
170	<sup>169</sup> Yb	177.2140(1)	6.4049(24)	170.8091(24)		
174	$^{169}{ m Yb}$	177.2140(1)	3.0221(20)	174.1919(20)		
187	<sup>169</sup> Yb	177.2140(1)	10.7538(6)	187.9678(6)	187.9669(3)	1.07
	$^{169}\mathrm{Yb}$	197.9579(1)	9.9913(5)	187.9666(5)		
	$^{182}\mathrm{Ta}$	179.3948(3)	8.5716(7)	187.9664(8)		
	$^{182}\mathrm{Ta}$	198.3530(3)	10.3865(8)	187.9665(9)		
193	<sup>169</sup> Yb	197.9579(1)	4.4549(47)	193.503(5)		
208	<sup>169</sup> Yb	197.9579(1)	10.2221(6)	208.1800(6)	208.1795(7)	1.73
	$^{182}\mathrm{Ta}$	198.3530(3)	9.8253(10)	208.1783(10)	20012100(1)	20
	$^{182}\mathrm{Ta}$	222.1099(3)	13.9366(54)	208.1733(54)		
217	$^{182}\mathrm{Ta}$	222.1099(3)	4.9583(15)	217.1516(15)	217.1519(20)	7.52
	$^{182}\mathrm{Ta}$	229.3220(6)	12.1734(10)	217.1486(12)	211.1010(20)	1.02
	<sup>233</sup> U	208.1795(7)	8.9754(8)	217.1549(11)		
240	$^{182}\mathrm{Ta}$	229.3220(6)	11.0473(30)	240.360(3)	940 9710(17)	1.94
210	$^{233}{ m U}$	245.3498(11)	4.9769(14)	$240.369(3) \ 240.3729(18)$	240.3719(17)	1.24
245	$^{182}\mathrm{Ta}$	229.3220(6)	16.0249(40)	245 247(4)	945 9409/11)	0.50
210	<sup>233</sup> U	248.7242(10)	3.3742(7)	$245.347(4) \ 245.3500(12)$	245.3498(11)	0.52
240	$^{182}\mathrm{Ta}$		, ,	` '		
248		264.0755(3)	15.3513(10)	248.7242(10)		
261	$^{182}\mathrm{Ta}$	264.0755(3)	2.1178(39)	261.958(4)		
268	<sup>182</sup> Ta	264.0755(3)	4.5992(21)	268.6747(21)		
274	$^{182}\mathrm{Ta}$	264.0755(3)	10.6580(14)	274.7335(14)	274.7347(13)	1.61
	$^{233}\mathrm{U}$	278.1080(9)	3.3718(13)	274.7362(16)		

TABLE V. (Continued).

<sup>233</sup> U	R	eference	${f Adopted}$	$\gamma$ -ray	y energy	
line	Nuclide	Energy	$\Delta E_{\gamma}$	Value	Average	$\chi^2_R$
278	$^{182}\mathrm{Ta}$	264.0755(3)	14.0326(11)	278.1081(11)	278.1080(9)	0.02
	$^{233}\mathrm{U}$	291.3561(9)	13.2483(14)	278.1078(17)	, ,	
288	<sup>233</sup> U	278.1080(9)	9.9209(9)	288.0289(13)	288.0292(9)	0.07
	$^{233}{ m U}$	291.3561(9)	3.3267(10)	288.0294(13)		
291	$^{169}\mathrm{Yb}$	307.7376(1)	16.3815(9)	291.3561(9)		
293	$^{169}\mathrm{Yb}$	307.7376(1)	13.7428(93)	293.995(9)		
302	$^{169}\mathrm{Yb}$	307.7376(1)	4.7471(44)	302.990(4)		
317	$^{169}\mathrm{Yb}$	307.7376(1)	9.4318(11)	317.1694(11)	317.1689(15)	2.04
	<sup>152</sup> Eu	344.2811(19)	27.1168(28)	317.1643(34)		
320	$^{169}\mathrm{Yb}$	307.7376(1)	12.8102(11)	320.5478(11)	320.5471(13)	2.32
	<sup>152</sup> Eu	344.2811(19)	23.7410(28)	320.5401(34)		
	<sup>233</sup> U	317.1689(15)	3.3782(4)	320.5471(16)		
323	$^{152}\mathrm{Eu}$	344.2811(19)	20.9013(27)	323.3798(33)	323.3806(14)	0.07
	$^{233}\mathrm{U}$	320.5471(13)	2.8337(9)	323.3808(16)		
328	$^{233}\mathrm{U}$	323.3806(14)	5.3779(44)	328.758(5)		
336	$^{152}\mathrm{Eu}$	344.2811(19)	7.6639(19)	336.6172(27)	336.6195(16)	1.06
	$^{233}\mathrm{U}$	323.3806(14)	13.2400(13)	336.6206(19)		
365	<sup>152</sup> Eu	344.2811(19)	21.5394(29)	365.8205(35)		
367	$^{152}\mathrm{Eu}$	344.2811(19)	23.5095(95)	367.791(10)	367.795(8)	0.41
	$^{233}\mathrm{U}$	365.8205(35)	1.9809(117)	367.801(12)		

<sup>&</sup>lt;sup>a</sup>Calculated uncertainty has been increased by a factor of 2 due to the large  $\chi_R^2$  value.

ample, the same spectra might be used to determine  $\Delta_2$  and, say,  $\Delta_3$ . Therefore,  $\Delta_2$  and  $\Delta_3$  would be correlated since the peak at  $E_2$  is common to both. Such least-squares fits have not been done, in part, because it is felt that any improvement in the  $\gamma$ -ray energies would not be significant.

In several instances in Table V, several values are averaged, with  $1/\sigma^2$  weighting, to obtain the final value. In most cases this weighting is not strictly correct since the individual values are often correlated, and this correlation has not been taken into account. For example, the average for the 187-keV  $\gamma$  ray involves energy differences with respect to the 177- and 197-keV lines from <sup>169</sup>Yb. These two values make use of the same  $\gamma$ -ray spectra and therefore the same 187-keV peaks. Thus, the two energy differences are not independent, and this is not taken into account in the calculation of the average. The effect of neglecting these correlations is that the computed uncertainty is smaller than it would be if the correlations were taken into account.

# IV. ENERGY RELATIONSHIPS IN 229Th

There are several interesting relationships among the energies of the  $\gamma$  rays in  $^{229}$ Th to be discussed before

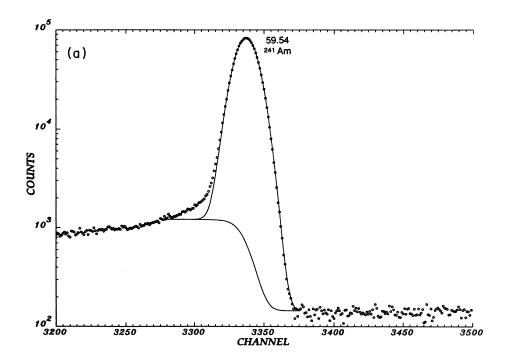
the energy of first excited state is determined. First, we should comment on the cascade-crossover relationship involving the first three levels in the ground-state rotational band. As shown in Fig. 1, this includes the 42- and 54-keV  $\gamma$ -ray cascade and the 97-keV crossover, involving the levels at 0, 42, and 97 keV. In our previous work [2] we did not use this relationship, even though these  $\gamma$  rays are among the strongest in the spectrum, because there was reasonable evidence that the observed 42-keV peak had two components.  $\gamma$ - $\gamma$  coincidence data [1] implied the existence a weaker 42-keV  $\gamma$  ray between the levels at 71.8 and 29.1 keV, although this  $\gamma$  ray was not directly observed. From the level energies deduced without use of the 42-keV lines, the energy of the weaker  $\gamma$  ray is 200 eV higher than that of the ground-state  $\gamma$ ray. Previous attempts to observe the doublet nature of the 42-keV peak were unsuccessful. However, with the improved resolution of the OR-16 detector, we have been able to observe a difference between the shape of the 42keV peak and those of the neighboring strong peaks. This is illustrated in Fig. 5, where Fig. 5(a) shows that the 59-keV peak from 241 Am is well fit by a Gaussian function, while Fig. 5(b) shows that the 42-keV peak deviates from a Gaussian function in a manner which implies the

<sup>&</sup>lt;sup>b</sup>Known doublet (see text), so the measured peak energy may vary with detector resolution.

existence of a second component on the high-energy side of the main peak. Since both of these peaks are in the same spectrum and have similar peak-to-continuum ratios, we are satisfied that the 42-keV peak is a doublet, and that the weaker component has the higher energy, as expected. Thus, we have not used any relationships involving the 42-keV  $\gamma$  in this work because the energy for this peak is different from that of the 42-keV  $\gamma$  ray to the ground state.

The remaining analysis depends critically on the correctness of the assumptions regarding the placement of those  $\gamma$  rays which, from spin-parity considerations alone,

would feed either the ground state or the first-excited state (energy= $\Delta$ ). In order to be able to deduce a realistic value for  $\Delta$ , each of these  $\gamma$  rays must populate only one of these levels with significant intensity. The choice of which of the two final states is populated by each of the E1 transitions has been discussed at length in Ref. [1]. It has been argued that the 71- and 29-keV transitions both terminate at the first-excited state. Since these are both intraband transitions, within the  $3/2^+[631]$  band, it is likely that most of the observed intensity in these two peaks does in fact correspond to this placement. However, the possibility exists that these two peaks may con-



10<sup>5</sup>
(b)
42.45

10<sup>2</sup>
2200
2250
2300
CHANNEL

FIG. 5. Gaussian fits to peaks at 59 keV, a singlet from <sup>241</sup>Am, and 42 keV, a doublet from <sup>233</sup>U.

tain some contribution from the transitions to the ground state. The magnitudes of such contributions to these two peaks have been calculated using reasonable values for the M1 matrix elements and the intrinsic quadrupole moment of the  $3/2^+[631]$  band, as discussed in Ref. [21]. There, it was estimated that the strengths of the ground-state transitions are smaller than those of the intraband transitions by factors of  $\sim 8$  and  $\sim 14$ , respectively, for the 71- and 29-keV peaks. These possible contributions are believed to be sufficiently small that their effects on the measured peak energies are not significant. Specifically, the energies of the  $\gamma$  rays to the level at  $\Delta$  should then be  $\sim 0.35$  eV lower than those of the corresponding doublet peaks.

As shown in Fig. 1, there are a few relationships among the  $\gamma$ -ray energies reported in Table V that can be used to provide checks on the quality or consistency of these results. In the relationships (see Sec. I) that were used to determine the energy of the <sup>229</sup>Th first excited state, the first two require that

$$E(71.8) - E(67.9) = E(29.1) - E(25.3).$$

From Table III, these two differences, as directly determined, are 3.8685(4) and 3.8701(4) keV, respectively. Although these two values differ by 0.0016(6) keV, more than the associated uncertainty, the agreement is satisfactory considering the weakness of the 25.3- and 67.9-keV peaks, as illustrated in Fig. 6 for the former  $\gamma$  ray. (The 29.1- and 71.8-keV lines are the ones that, from spin-parity considerations, potentially could be doublets, with components feeding both the 0- and  $\Delta$ -keV levels.)

There are two cascade-crossover combinations that can also be used to test the consistency of the  $^{233}$ U  $\gamma$ -ray energies. These combinations are the 217.1=187.9+29.1 and 164.5=135.3+29.1, as shown in Fig. 1. The corresponding differences between the cascade and crossover

TABLE VI. Difference between crossover and cascade energies.

$\gamma$ rays (keV)	Difference (keV)
217-187-29	+0.0004(36)
164-135-29	+0.0001(31)

energies are shown in Table VI. Both of these values are consistent with zero. However, their uncertainties are dominated by that of the 29-keV line, which is 0.0030 keV. One can turn the argument around and, assuming that these two relationships must be zero, use them to deduce values for the energy of the 29-keV  $\gamma$  ray. Doing this, one finds that the two resulting values are 29.1850(20) and 29.1847(7) keV, and their average is 29.1847(7) keV. This value agrees extremely well with the measured value of 29.1846 keV, but the uncertainty is smaller by a factor of  $\sim$  4. Then, from the 25U-29U difference in Table III, one can use this deduced energy value to obtain a value of 25.3146(8) keV for the energy of the 25-keV line.

From the  $\gamma$ -ray energies that we have determined, there are four energy combinations that can be used to obtain the energy of the first-excited level in <sup>229</sup>Th. These relationships are shown in Fig. 1. The energies from these combinations are shown in Table VII. All four values show a positive energy for this level, in contrast to the result of Ref. [2], where two of the three combinations gave negative values. For the first two relations, two values are given—one from the values in Table V for  $E_{\gamma}(25)$  and  $E_{\gamma}(29)$  and the other from the values deduced in the previous paragraph for these two lines.

Several average values are given in Table VII. The unweighted averages are given to show the influence of the weight resulting from the smaller uncertainty for the value of 0.0036(6) from the third relation. The last line gives the weighted averages based on the uncertainties given.

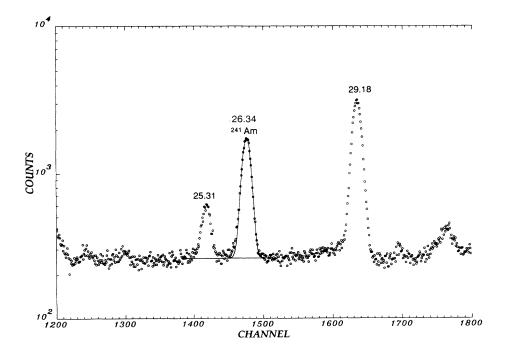


FIG. 6. Portion of the  $^{233}$ U and  $^{241}$ Am  $\gamma$ -ray spectrum measured with the OR-16 detector showing the weak 25-keV line.

TABLE VII. Energy,  $\Delta$ , of the first excited level of <sup>229</sup>Th.

		Δ (keV	)	
	Set 1 <sup>a</sup>	•	Set 2 <sup>b</sup>	
$\gamma$ rays (keV)	Energy	$\chi^2_R$	Energy	$\chi^2_R$
97-71-25	+0.0069(22)		+0.0029(22)	
97-67-29	+0.0028(31)		+0.0027(9)	
[148-146]-[118-117]	+0.0036(6)			
[148-146]-[76-74]	+0.0029(10)			
Unweighted average	+0.0040(10)		+0.0030(2)	
Weighted average	$+0.0036(5)^{'}$	0.93	+0.0032(4)	0.29

<sup>&</sup>lt;sup>a</sup>The energies for  $E_{\gamma}(25)$  and  $E_{\gamma}(29)$  are from Table V.

#### V. RESULTS AND DISCUSSION

From the results in Table VII, we have adopted an energy of 3.5(10) eV for the first excited state of <sup>229</sup>Th. This value has been taken from the two averages in the last line of Table VII, with the uncertainty increased by a factor of 2 to allow for any unidentified systematic errors.

We now have for the first time a value from  $\gamma$ -spectroscopic studies which excludes zero for the energy of the first-excited state in <sup>229</sup>Th. This level has also been reported in (d,t)-reaction studies [9,22], where it was identified as a relatively weak peak, unresolved from the ground state, in the triton spectrum. These latter studies could not answer the question of what the energy of the state was, except to show that it was within a few keV of the ground state.

Knowledge of the half-life of this state would be of considerable interest. We presently have no direct measurement of this quantity. Since a  $\gamma$  transition connecting this state and the ground state must be pure M1 (at this energy, any E2 admixture would be vanishingly small) and since the wavefunctions of both states are presumably known, the  $\gamma$ -ray lifetime can in principle be obtained by direct calculation. However, the M1 transition is asymptotically hindered, and different values chosen for the parameters of the nuclear potential well give rather different values for this transition probability, as discussed previously [21]. However, a transition between these same two Nilsson states is observed as a prominent 312-keV  $\gamma$  ray in <sup>233</sup>U, following the  $\beta^-$  decay of <sup>233</sup>Pa. The half-life of this 312-keV level is known, and hence the B(M1) value of this  $3/2^+[631] \rightarrow 5/2^+[633]$  transition can be determined. This "experimental" B(M1) value is found to be  $0.0060\mu_N^2$ . From this, the  $\gamma$ -ray half-life of this level in  $^{229}$ Th is calculated to be  $\sim 45$  h for a 3.5-eV M1 transition. With account taken of the  $\pm 1$  eV uncertainty in the excited-state energy, this half-life could be as long as  $\sim 120$  h or as short as  $\sim 20$  h.

It needs to be borne in mind, however, that this is almost certainly not the actual half-life of this level. The overall level half-life will most likely be determined primarily by the interaction of the electronic structure with the nucleus. Because of the uniquely small value of the excited-state energy, this interaction should be especially sensitive to the outermost electrons, which are the ones most affected by the chemical and physical environment. We thus expect that the 3.5-eV level may not have a unique "half-life" at all, but rather that the value measured for this quantity will depend on the physical and chemical properties of the sample containing the <sup>229</sup>Th. Studies, both experimental and theoretical, of such a phenomenon promise to provide interesting new insights into atomic and condensed-matter physics.

#### **ACKNOWLEDGMENTS**

The authors wish to acknowledge the assistance of the staff of the Radiation Measurements Laboratory for the use of a counting room and for assistance in optimizing the electronics. They also wish to thank E. W. Killian for modifications of the GINA spectral analysis program, J. D. Baker for preparing most of the sources used, K. D. Watts for assisting with the measurements, and R. C. Greenwood for comments on the manuscript. This research was supported by the U.S. Department of Energy through the EG&G Idaho Laboratory Directed Research & Development Program, under DOE Field Office, Idaho Contract No. DE-AC07-76IDO1570.

<sup>&</sup>lt;sup>b</sup>The energies for  $E_{\gamma}(25)$  and  $E_{\gamma}(29)$  are derived in the text from the computed 217-187 and 164-135 differences for the 29 line and from the measured 29-25 (Table III) difference for the 25 line.

L. A. Kroger and C. W. Reich, Nucl. Phys. A259,
 (1976); L. A. Kroger, Ph.D. thesis, University of Wyoming, 1971 (unpublished).

<sup>[2]</sup> C. W. Reich and R. G. Helmer, Phys. Rev. Lett. 64, 271 (1990).

<sup>[3]</sup> V. F. Strizhov and E. V. Tkalya, Zh. Eksp. Teor. Fiz. 99,

<sup>697 (1991) [</sup>Sov. Phys. JETP 72, 387 (1991)].

<sup>[4]</sup> E. V. Tkalya, Pis'ma Zh. Eksp. Teor. Fiz. 55, 216 (1992)[JETP Lett. 55, 211 (1992)].

<sup>[5]</sup> F. F. Karpeshin, I. M. Band, M. B. Trzhaskovskaya, and B. A. Zon, Phys. Lett. B 282, 267 (1992).

<sup>[6]</sup> E. V. Tkalya, in Proceedings of the III International

- Symposium on Weak and Electromagnetic Interactions, WEIN-92, Dubna, 1992 (unpublished).
- [7] E. V. Tkalya, Yad. Fiz. 55, 2881 (1992) [Sov. J. Nucl Phys. 55, 1611 (1992)].
- [8] S. Wycech and J. Zylicz, Frontier Topics in Nuclear and Astrophysics (IOP, Bristol, 1992), p. 365.
- [9] D. G. Burke, P. E. Garrett, Tao Qu, and R. A. Naumann, Phys. Rev. C 42, R499 (1990).
- [10] R. G. Helmer, R. J. Gehrke, and R. C. Greenwood, Nucl. Instrum. Methods 123, 51 (1975).
- [11] R. G. Helmer and C. W. Reich, U.S. DOE Report No. EGG-NRP-10693, 1993.
- [12] R. G. Helmer, P. H. M. Van Assche, and C. van der Leun, At. Data Nucl. Data Tables 24, 39 (1979).
- [13] E. G. Kessler, R. D. Deslattes, A. Henins, and W. C. Sauder, Phys. Rev. Lett. 40, 171 (1978).
- [14] R. G. Helmer, Nucl. Instrum. Methods A 330, 434 (1993).

- [15] R. G. Helmer, A. J. Caffrey, R. J. Gehrke, and R. C. Greenwood, Nucl. Instrum. Methods 188, 671 (1981).
- [16] B. Jeckelmann, W. Beer, G. De Chambrier, O. Elsenhans, K. L. Giovanetti, P. F. A. Goudsmit, H. J. Leisi, and A. Rüetschi, Nucl. Instrum. Methods A241, 191 (1985).
- [17] R. D. Deslattes, E. G. Kessler, W. C. Sauder, and A. Henins, Ann. Phys. (N.Y.) 129, 378 (1980).
- [18] E. K. Warburton and D. E. Alburger, Nucl. Instrum. Methods A 253, 38 (1986).
- [19] G. C. Nelson and B. G. Saunders, Nucl. Instrum. Methods 84, 90 (1970).
- [20] R. W. Jewell, W. John, R. Massey, and B. G. Saunders, Nucl. Instrum. Methods 62, 68 (1968).
- [21] C. W. Reich, Izv. Akad. Nauk SSSR, Ser. Fiz. 55, 878 (1991).
- [22] J. R. Erskine (private communication), also quoted in Y. A. Akovali, Nucl. Data Sheets 58, 555 (1989).